TECHNICAL MEMORANDUM

532

Selection of IASI Channels for Use in Numerical Weather Prediction

A.D. Collard

Research Department

July 2007

European Centre for Medium-Range Weather Forecasts
Europäisches Zentrum für mittelfristige Wettervorhersage
Centre européen pour les prévisions météorologiques à moyen terme

Series: ECMWF Technical Memoranda

A full list of ECMWF Publications can be found on our web site under:
http://www.ecmwf.int/publications/

Contact: library@ecmwf.int

Abstract

IASI (Infrared Atmospheric Sounding Interferometer) is an infrared Fourier transform spectrometer flying on the MetOp satellite series starting in October 2006. It measures the radiance emitted from the Earth in 8461 channels covering the spectral interval from 645–2760cm^{-1} at a resolution of 0.5cm^{-1} (apodised). The high volume of data resulting from IASI presents many challenges, particularly in the areas of data transmission, data storage and assimilation.

The simplest methods for reducing the data volume are spatial sampling and channel selection. The issue of channel selection is discussed and a selection of 300 channels suitable for tranmission to NWP centres is examined, where the primary aim is the improvement of the temperature, humidity, ozone and carbon dioxide state vectors. The channel selection method takes account of redundancy, the effect of interfering species and robustness against the choice of assumed background error covariance and atmospheric state.

1 Introduction

The first of the IASI (Infrared Atmospheric Sounding Interferometer) series (Chalon *et al.*, 2001) was launched on the MetOp-A satellite on 19$^{\text{th}}$ October 2006. IASI is an infrared Fourier transform spectrometer and as part of the EUMETSAT European Polar System (EPS) is the first such instrument to be designed for operational meteorological measurements.

IASI measures the radiance emitted from the Earth in 8461 channels covering the spectral interval from 645–2760cm^{-1} at a resolution of 0.5cm^{-1} (apodised) and with a spatial sampling of 18km at nadir. The high volume of data resulting from IASI presents many challenges, particularly in the areas of data transmission, data storage and assimilation.

The selection of a subset of channels is an established method for reducing the amount of data to be assimilated for each IASI field of view. Distribution and assimilation of selected channels is the current operational configuration for AIRS — the first high spectral resolution infrared sounder to be assimilated into NWP models.

This report describes a methodology for the selection of a subset of 300 IASI channels that may be distributed such that the total loss of information is a minimum. The value of 300 was chosen as this is the likely maximum number of IASI channels suitable for distribution by EUMETSAT via the Global Telecommunications System. The same approach (and the channels selected) is also applicable to choosing a subset of channels to be assimilated.

A number of techniques have been suggested for channel selection for high spectral resolution infrared sounders and these are reviewed and compared in Rabier *et al.* (2002) where they conclude that the channel selection method of Rodgers (1996, 2000) is the most optimal (for a static, rather than dynamic, channel selection).

Section 2 describes the channel selection method and discusses the choices that may be made at the various stages of the process. Section 3 then describes a practical implementation of the channel selection process for the specific aim of a general NWP selection of 300 channels. Section 4 reviews the selection of Section 3. Conclusions make up Section 5.

2 Overview of the method.

Before setting up the channel selection process we first need to identify the atmospheric properties for which information is to be preserved, as the exact content of a selected set of channels will be highly dependent on the precise application to which it is being applied. For the purpose of NWP the information we aim to preserve in the channel selection relates to profiles of temperature, humidity, ozone, carbon dioxide and the surface temperature.

As techniques and modelling accuracy evolve, the “optimal” set of channels will also change. However, one must also consider that two very different channel selections may contain very similar information. Therefore, the aim with this approach is not to produce an absolutely “optimal” set of channels, as this is almost certainly not possible for all applications. Here we select a conservative and close to optimal set of channels for extracting atmospheric information for NWP.

In order to infer the above quantities, auxiliary knowledge of cloud properties and surface emissivity is necessary. These may also be inferred from the IASI observations and channels necessary for this purpose need to be chosen.

On choosing channels it should be remembered that shortwave channels ($\lambda < 5\mu$m) can be affected by sunlight. Although current state of the art radiative transfer models such as RTIASI-5 (Matricardi, 2004) have the capability to model solar contaminated observations well, it is still more challenging to use these wavelengths (especially in the presence of cloud or aerosol), and they should not be chosen in preference to longwave channels that can provide similar information. Also, water vapour and ozone channels should not be the primary providers of temperature information as their temperature Jacobians can be highly state-dependent. Therefore at different stages of the channel selection process different sets of channels are considered.

The channel selection method presented here consists of three main stages:

1. Removal of channels based on *ad hoc* criteria to avoid spectral regions with large uncertainties in the modelled spectra (i.e., pre-screening).

2. The main selection algorithm based on the information content of the measurements. This is comprised of a number of individual selection runs.

3. *Ad hoc* addition of channels for specific purposes that could not be represented by the information content based selection algorithm.

The following three sections discuss possibilities for pre-screening (Section 2.1), the selection of channels (Section 2.2) and additional *ad hoc* channel selection (Section 2.3). A number of possible courses of action are discussed. The practical implementation of the selection algorithm is presented in Section 3.

2.1 Approaches to Pre-screening

The channel selection method described should avoid channels with large forward model uncertainty. Here a variety of approaches that may be considered for pre-screening are discussed. This is intended as an overview of all the possible pre-screening issues and for practical reasons not all of the following are considered in the actual channel selection runs (see Section 3).

1. Consideration of channels that are significantly dominated by trace species (i.e., minor species whose impact on the spectrum cannot be modelled with sufficient accuracy due to uncertainty in their abundances or spectroscopy). This may be achieved through radiative transfer calculations where species abundances in the radiative transfer model are varied by their climatological range (for various representative test atmospheres) and any channel showing variation by more than the IASI instrument noise level is rejected. However, for some species (e.g., CH_4) this might result in an unacceptably high rejection rate (thousands of channels) and

the criterion might need to be relaxed (but with the assumed forward model error adjusted accordingly). Conversely, some species might have a correlated spectral signal that, while below instrument noise level for a single channel, becomes significant when considered for the spectrum as a whole. The information on random noise contributed by trace species for un-rejected channels should be included in the estimate for the forward model error covariance matrix.

2. Consideration of inter-comparison exercises. Inter-comparison exercises such as LIE (Tjemkes *et al.*, 2003) and Rizzi *et al.* (2002) and the various AIRS validation studies can be used to identify areas in the spectrum where the radiative transfer calculations are particularly problematic. J. Taylor (priv. comm.) has, for example, identified spectral lines in the 6.3μm water vapour band that appear to have erroneous spectroscopy in the line databases.

The LIE study includes comparisons between different radiative transfer models and between these models and existing observed high spectral resolution infrared observations (plus measurements of the associated atmospheric state), thus highlighting spectral regions where there is disagreement in forward modelling.

3. NWP monitoring statistics. Comparisons between observed radiances and simulated radiances from short-range forecast fields can identify possibly problematic channels which might necessitate changes to the channel selection. The current experience with AIRS can identify many such channels (e.g., the high-peaking channels around 4.3μm which are highly influenced by unmodeled non-LTE effects) but AIRS does not cover the same spectral range nor does it have the same spectral resolution as IASI. If post-launch monitoring of IASI does identify bad channels, they may either be substituted for good ones (if such a change is not too late) or advice may be distributed on the use of these channels (as is current practice with satellite measurements).

In summary, channels should be avoided if they have large sensitivity to radiative transfer model errors; are sensitive to variable species whose variability is not considered in the background or on analysis; or which have known radiative transfer weaknesses.

2.2 Selection Methodology

After pre-screening, the selection of channels is performed.

The channel selection is based on the methodology suggested by Rodgers (1996, 2000). This method was shown to be the best method for *a priori* determination of an optimal channel set by Rabier *et al.* (2002) and has been further evaluated in the context of AIRS by Fourrié and Thépaut (2003).

The method relies on evaluating the impact of the addition of single channels on a figure of merit and proceeds as follows:

1. Test which single channel most improves a chosen figure of merit. This figure of merit is normally a quantity reflecting the improvement of the analysis error covariance matrix, $\mathbf{A}$, over the background error covariance matrix, $\mathbf{B}$. Therefore, starting with $\mathbf{A}_0$=$\mathbf{B}$ (where $\mathbf{A}_i$ is the analysis error covariance matrix after i channels have been chosen), the possible values of $\mathbf{A}_i$ for each chosen channel will need to be calculated.

2. After the optimal $\mathbf{A}_i$ has been determined through the choice of the best new channel, find the remaining channel that most improves the figure of merit.

3. Repeat until a sufficient number of channels have been selected.

Rodgers speeds this process up by noting that, if the instrumental noise plus forward model error covariance matrix is diagonal[1], on adding a new channel, i, to the analysis, the solution error covariance is changed from

[1] Theoretically, a realistic estimate of the full error covariance matrix would be desirable, even though the channel selection calcu-

$\mathbf{A}_{i-1}$ to $\mathbf{A}_i$ thus:

$$\mathbf{A}_i = \mathbf{A}_{i-1}\{\mathbf{I} - \mathbf{h}_i(\mathbf{A}_{i-1}\mathbf{h}_i)^{\mathrm{T}}/[1+(\mathbf{A}_{i-1}\mathbf{h}_i)^T\mathbf{h}_i]\}.$$

Here $\mathbf{h_i}$ is the Jacobian for channel *i* normalised by the standard deviation of the instrument plus forward model noise for that channel.

In this scheme, the degrees of freedom for signal (DFS) for the assimilation ($\mathrm{Tr}(\mathbf{I} - \mathbf{AB^{-1}})$) is used as the figure of merit. An alternative is the entropy reduction ($-0.5\ln|\mathbf{AB}^{-1}|$) but past experience (e.g., Rabier *et al.*, 2002) has shown that the differences between choosing DFS or entropy reduction are small. Required for this method are an estimate of the background error covariance matrix (the ECMWF NWP background error covariance matrix operational from Jan. 2003 – Jun. 2005, modified for use in a 1DVar scenario), an estimate of the observational error covariance matrix (including forward model errors), and a forward model to estimate the Jacobians for the atmospheres being considered (RTIASI-4: Matricardi and Saunders, 1999; Matricardi, 2003). Usually, the process is applied to the case of a single atmospheric profile, but may be extended to consider, simultaneously, multiple profiles.

As the effect of the precise atmospheric profiles used on the final selection may be important (Rabier et al., 2002), the final channel selection should be tested against the optimal selection for a diverse range of atmospheric profiles.

The method is then implemented as follows:

1. Take the IASI channels that remain after pre-screening

2. Choose a range of atmospheric scenarios: the six AFGL standard atmospheres or part of the ECMWF atmospheric database (Chevallier, 1999; Chevallier *et al.*, 2000), for example. Consider these different scenarios simultaneously, so that, while the **A** and **B** matrices themselves are calculated independently, the total DFS for all the profiles is used as the figure of merit (one may also weight each individual profile by the inverse of the total achievable DFS as in Lipton, 2003). The reason for this is to ensure that channels are chosen based on the combined requirements of the range of atmospheres.

3. To ensure that temperature information is primarily coming from the relatively linear[2] CO_2 channels, start by ignoring those channels that are most sensitive to water vapour or ozone (based on the sensitivity of the IASI radiances to realistic variations in the water vapour or ozone abundance). Also, pre-screen those channels that are sensitive to solar irradiance; as it should be ensured that the channel selection does not rely on channels that cannot be used in the daytime.

4. Perform the above analysis for temperature, using the channels that remain. The number of channels that are chosen is determined by consideration of the total number that are required and the amount of DFS that is explained as a function of the total for all the channels being considered. This choice will necessarily be somewhat subjective

5. With the temperature channels chosen above pre-selected, perform the DFS analysis once more with the water vapour channels included and with both water vapour and temperature assimilation allowed. Further channels are thus chosen which are primarily sensitive to humidity but which will also contribute further temperature information.

5a. Optionally repeat the above for trace gas (O_3, CO_2, CH_4, CO, N_2O, etc.) assimilation, if required.

lations would be slowed signifi cantly. This matrix is, however, very diffi cult to estimate and, furthermore, for various practical reasons the assumed error covariance matrix is often very conservative and very different from the true matrix. With these considerations in mind, it is practically more sensible to consider a reasonable diagonal matrix. The impact of this assumption has not been determined and is beyond the scope of this report.

[2] Linear in this context refers to the case where the temperature Jacobian is not sensitive to realistic variation in the absorber amounts.

6. Repeat steps 3 and 4, but include the solar-affected channels.

The channel selection process is normally stopped either once a pre-selected number of channels is reached or once the improvement on adding new channels is relatively small. In the above method both criteria will be used and there will necessarily be some subjective choices to be made.

2.3 Selection of Additional Channels.

The selection of channels useful in the determination of cloud properties and surface emissivity, if this is required, is probably best done through manual selection of channels (if suitable ones are not already in the above dataset) on consideration of the spectral properties being considered. This approach or alternative automatic approaches (e.g., Crevoisier *et al.*, 2003) may also be preferable for trace gases (rather than step 5a above) as our knowledge of the B-matrices for these is often poor.

3 A Practical Selection of 300 IASI Channels for NRT distribution to NWP Centres.

In this section an example of the channel selection method is given where a total of 300 channels are chosen. This is an example with a diagonal combined observation and forward model error covariance matrix, where the forward model error is 0.2K plus the effect of trace gases only. The selection of channels for the assimilation of trace gases (i.e., all species except water vapour, ozone and carbon dioxide) is not performed.

3.1 Pre-screening.

The channels which are initially removed on pre-screening (“blacklisted channels”) are shown in Figure 1. Channels are removed if the effect on the brightness temperature due to climatological variability is greater than 1K for any of the six AFGL standard atmospheres. Ten species were examined in this way (CH_4, CO, N_2O, CCl_4, CFC-11, CFC-12, CFC-14, HNO_3, NO_2, OCS, NO, and SO_2) but only the first three had large enough effects for blacklisting. If a species has an impact lower than 1.0K, its effect is added to the forward model error covariance matrix. CO_2 has been assumed to have a constant abundance in this example (although variability in its abundance can cause variations in the observed brightness temperature of up to around 0.5K in the 15μm band), as much of its variability can probably by removed through bias correction or the use of a climatological mean (e.g., Engelen *et al.*, 2001).

Channels applicable to the assimilation of trace gas abundances are not chosen explicitly. It is suggested that trace gas channels may be added with reference to techniques developed specifically for this purpose (e.g., Crevoisier *et al.*, 2003).

Additionally shown in Figure 1 are those channels which are significantly influenced by the surface, by water vapour, by ozone and by solar irradiance. Some or all of these channels are removed in “pre-selection” runs.

3.2 Information content based channel selection.

The assumed instrument plus forward model error is shown in Figure 2. The instrument noise is measured level 1c flight model instrument noise as supplied in November 2004 (Phulpin, *priv. comm.*); the forward

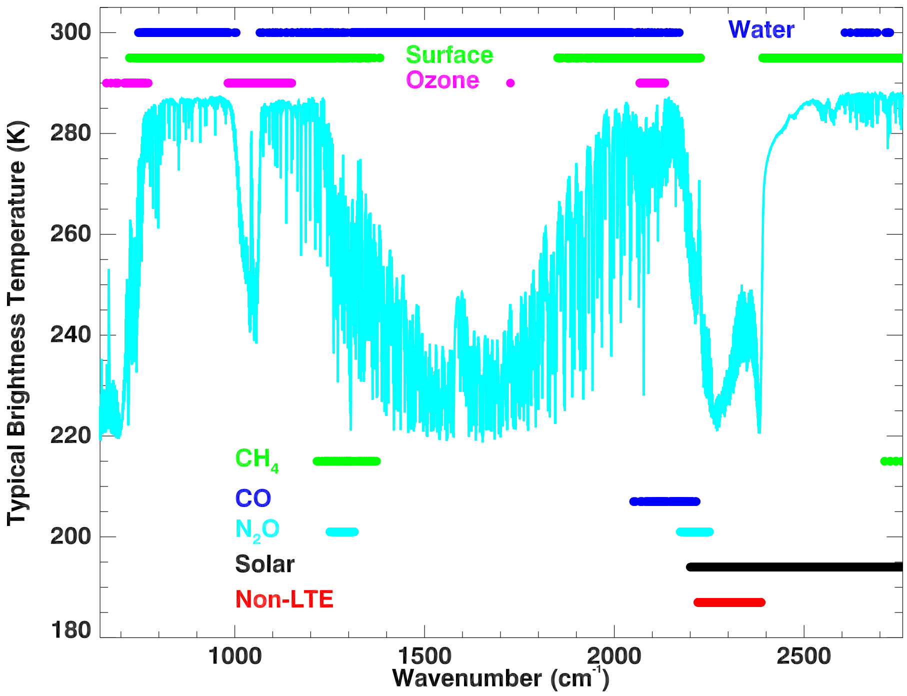

Fig. 1. Blacklisted channels for channel selection. Channels with possible signals from CH_4*, CO or* N_2O *greater than 1K are blacklisted together with those channels in the 4.3μm* CO_2 *band which are affected by non-LTE effects. Channels with large contributions from* H_2O*,* O_3*, the surface and solar irradiance are also indicated.*

model noise is taken to be a constant 0.2K plus estimates of the error due to the variability of trace gases. In this case the combined instrument and forward model error covariance matrix is assumed to be diagonal. The instrument noise is assumed to be constant in radiance space and thus varies with scene temperature in brightness temperature space, the 0.2K forward model noise is assumed to be constant in brightness temperature space.

The background error covariance matrix assumed is based on the operational ECMWF background error covariance matrix. The standard deviations for this matrix are shown in Figure 3.

This channel selection is based on the six AFGL standard atmospheres and view angles of 0° (nadir) and 40°. Degrees of freedom for signal (DFS) is used as the figure of merit. As interchannel error correlations are not accounted for and the IASI level 1c data are apodised (and thus have highly correlated errors between adjacent channels), a channel cannot be chosen if one of its immediate neighbours is already chosen.

This channel selection is performed in seven stages:

1) An initial run is performed with only the temperature analysis being considered and with the water vapour, ozone and solar channels excluded (in addition to the blacklisted channels, of course). This is to ensure that a minimum amount of temperature information is derived from CO_2 channels rather than H_2O and O_3 channels (as in a linear analysis the dependence of the temperature Jacobians on H_2O and O_3 amount is not accounted for). Solar channels are excluded to ensure that this set is usable in the daytime as well as night. Approximately 55% of the total degrees of freedom for signal (considering temperature only) are obtained with the first 30 channels.

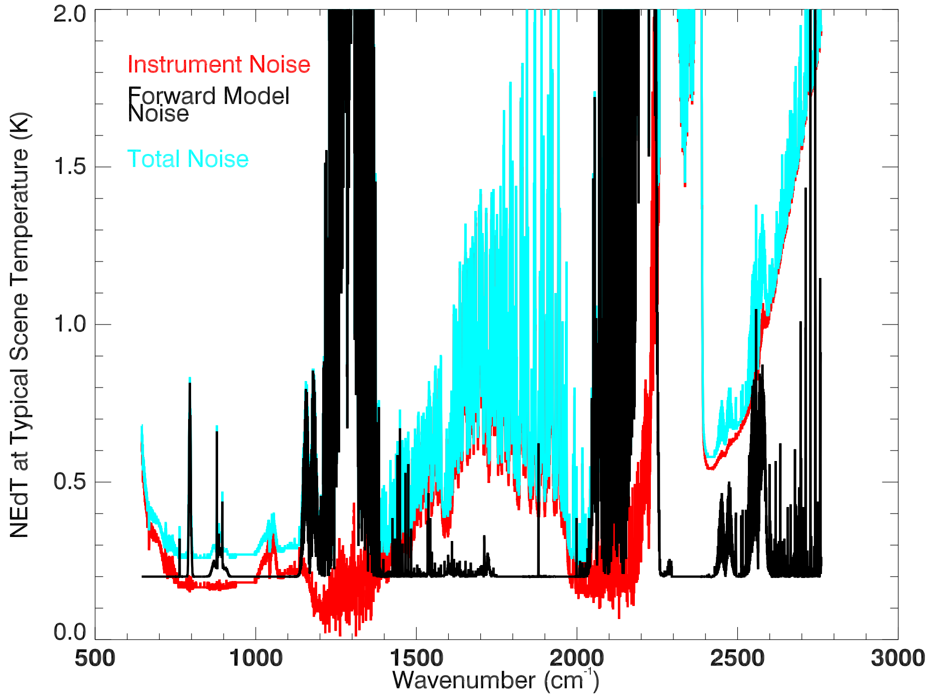

Fig. 2a: The assumed observational plus forward model noise as used in the channel selection for the AFGL U.S. Standard Atmosphere.

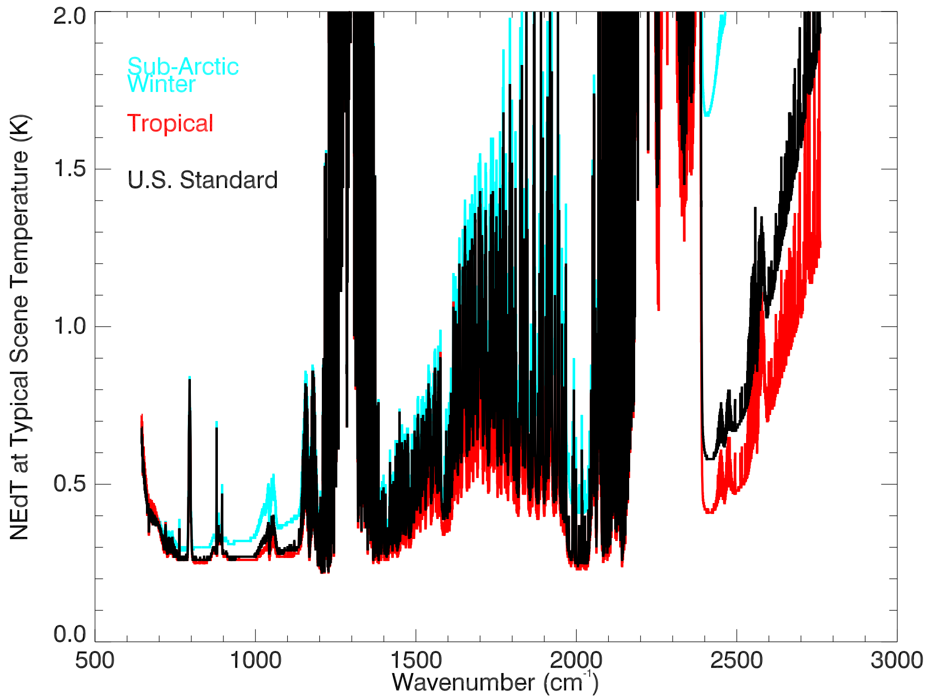

Fig. 2b: Variability of the assumed noise with different AFGL standard atmospheres.

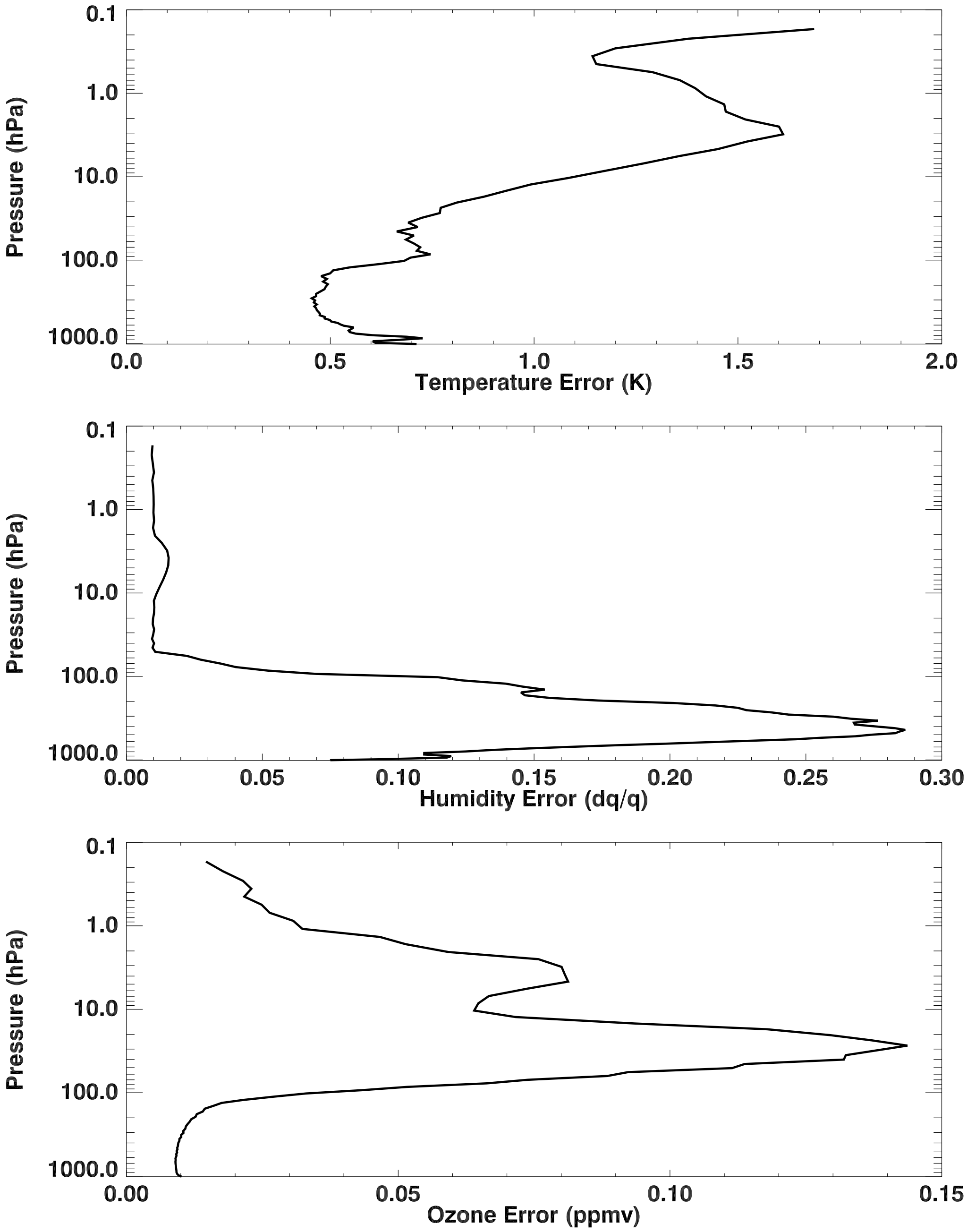

Fig. 3: Standard deviations of temperature, humidity and ozone taken from the operational ECMWF background error covariance interpolated onto the 90 RTIASI levels. A skin temperature error of 2.0K is assumed.

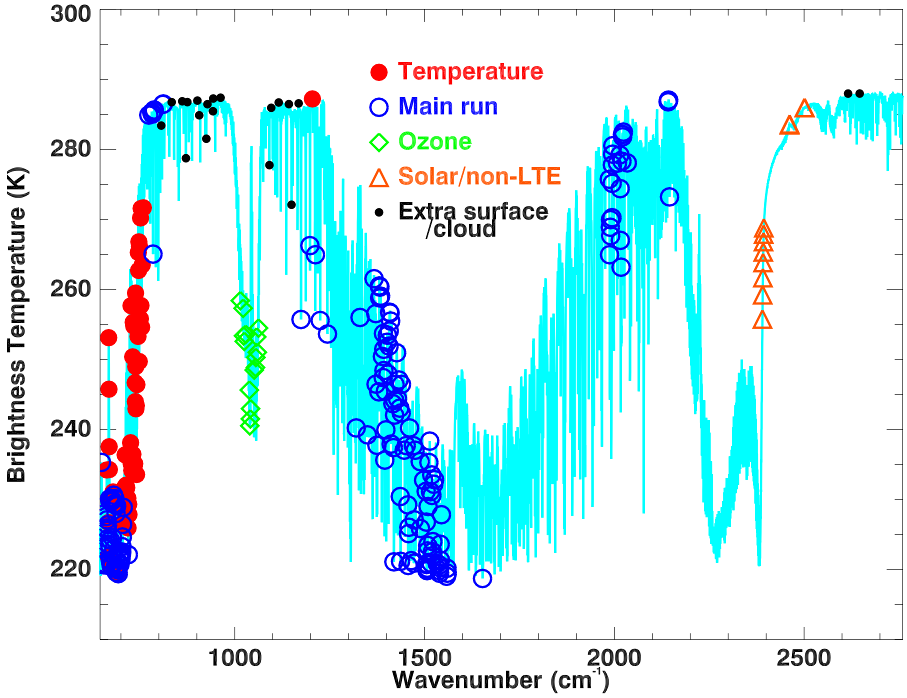

Fig. 4. 300 channels chosen with the methodology described in the text.

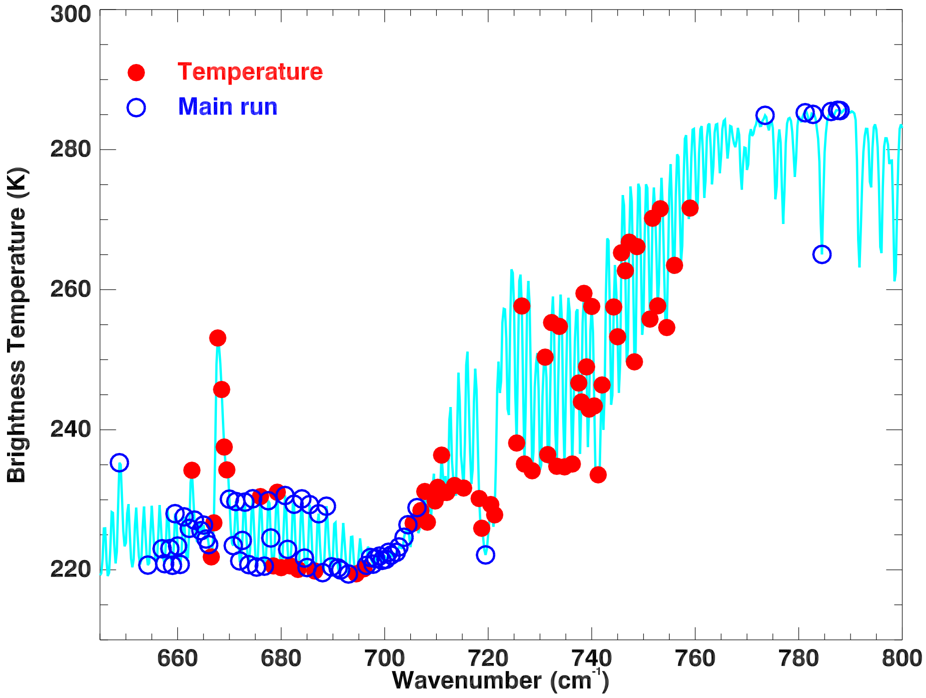

Fig. 5: As Figure 4, except focusing on the 15μm CO_2 *band.*

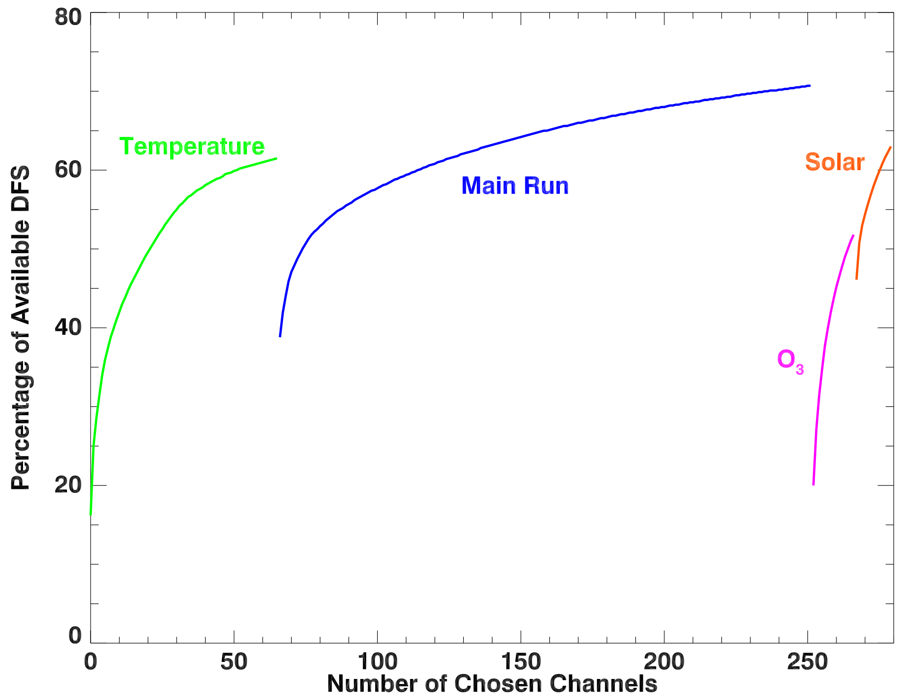

Fig. 6: Evolution of the DFS during the channel selection. The "available DFS" is derived for temperature assimilation only, temperature and humidity assimilation, ozone assimilation only; and temperature and humidity assimilation when using channels with wavelengths less than 5μm only.

2) Following the ECMWF experience with AIRS (G. Kelly, *priv. comm.*), it is expected that a large fraction of the total forecast impact from IASI will come from the upper tropospheric temperature sounding channels in the 15μm CO_2 band. Therefore, an additional step is introduced to ensure a maximum number of such channels are included in the final selection (while preserving the restriction on adjacent channels). An additional 36 channels in the range 250–460 (707.25–759.75cm^{-1}) with temperature jacobian peaks in the troposphere are thus chosen. These channels increase the fraction of the total temperature degrees of freedom to 62%.

3) Taking the 66 pre-selected channels from the first stage, the channel selection is now preformed with water vapour being considered in addition to temperature and with the water vapour channels included. 252 channels (including the 66 pre-selected ones) are chosen. The total available DFS in this case is 168.0 (i.e., an average of 14.0 per profile) of which 118.8 (71%) is obtained with the 252 channels.

4) Next the channels from stage 3 are preselected and ozone analysis is allowed. For this step the analysis is for ozone only (i.e., the temperature and water vapour profiles are assumed to be known). The total DFS for ozone is 23.0 (1.9 per profile); 52% of this DFS is accounted for with the 15 ozone channels that are chosen.

5) Allow the solar irradiance-affected channels to be used. Unfortunately, the noise in these channels is so high that channels in the longwave part of the spectrum are still selected in preference to the shortwave. As for research purposes, these channels might still be of interest, 13 channels were chosen when wavelengths below 4.189μm were considered *only* (this value being chosen to avoid channels which suffer from non-LTE effects. The total DFS when considering this spectral region is only 20.3 (1.7 per profile) and the 13 channels chosen account for 63% of it.

6) Taking the channels from the previous steps, allow carbon dioxide analysis. As with ozone, the analysis is for CO_2 only — the other quantities are assumed to be known. A simple diagonal background error covariance is assumed with a constant standard deviation of 10ppmv. The total DFS in this case is 16.3 (1.36 per profile) and 59.7% of this is already explained by the channels already chosen. No additional CO_2 specific channels are added, therefore.

7) In order to allow for derivation of surface emissivity and cloud properties, 20 additional window channels and channels on weak absorption lines in the window are added. The use of weak absorption lines in the derivation of surface and cloud emissivity is discussed in Huang *et al.* (2004).

The chosen channels are shown in Figures 4 and 5 and the evolution of the DFS is shown in Figure 6.

4 Discussion of Results.

This section reviews the channel selection and investigates its robustness against the choice of profiles and background error covariance.

4.1 Some notes on the channels chosen.

Many channels are chosen in the 670–710cm^{-1} region which are sensitive to the temperature of the upper troposphere and lower stratosphere. This is partially a reflection of the relatively high *a priori* temperature errors in this region, compared to the troposphere, but also reflects the somewhat higher instrument noise levels for these channels.

Very few surface sounding channels are chosen as the skin temperature variance is reduced by over an order of magnitude by the very first surface sounding channel chosen. This is a result of the forward model error not including the highly correlated errors resulting from emissivity uncertainty and undetected cloud. This deficiency has been addressed by the manual inclusion of extra window channels in Step 7 above.

Figures 7 and 8 compare this IASI channel selection with the 324 channels chosen for near-real time distribution from AIRS. However, it is hard to make a direct comparison as the AIRS channels do not have exactly the same frequencies as the IASI ones; the instrument spectral response functions differ; the instrument noise characteristics are different; the shortwave portion of the 6.3μm water vapour band is not measured by AIRS and the criteria for choosing these channels was different.

Another consideration of the utility of the channel selection is whether the Jacobians of the selected channels are sufficiently localised. In particular if channels sensitive to the troposphere have high sensitivity to the state of the atmosphere in the upper stratosphere or above, large errors in the upper level model temperature fields can compromise the accuracy of the information being provided lower down.

Figures 9a and 9b show for the main temperature and water vapour sounding regions of the spectrum the impact of a 1K temperature perturbation for all levels above 10hPa on the observed brightness temperature as a function of the level of the Jacobian peak for each channel. The red dots are the channels in this selection, the green dots are those channels available for selection but not chosen; and the small black dots are blacklisted channels. It can be seen that the channels chosen are generally either as good as the channels that were omitted or, in the case of the water vapour, often significantly better.

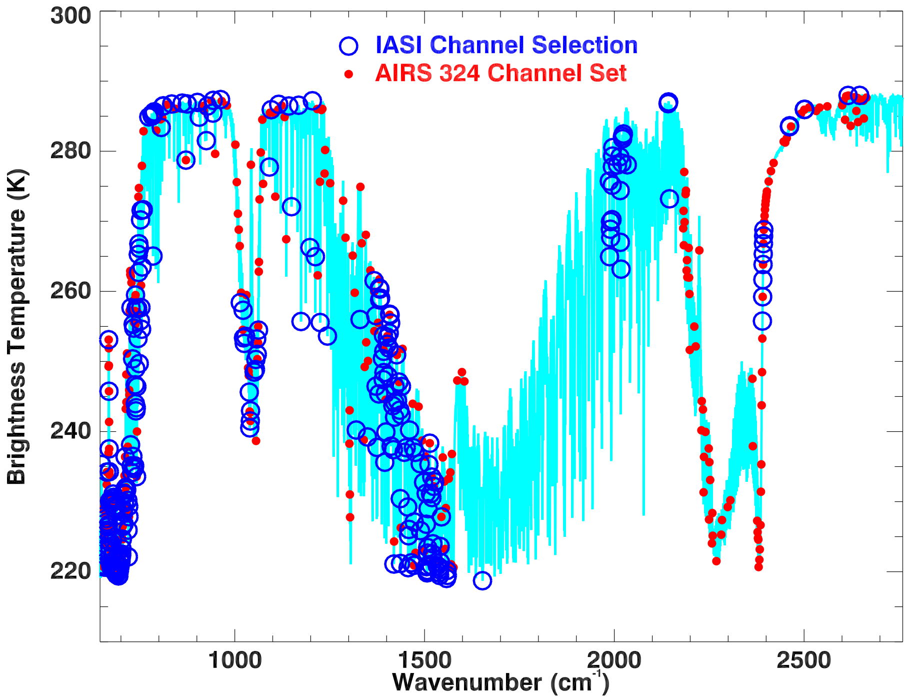

Fig. 7: A comparison of the 324 channels distributed for AIRS and the 300 channels chosen for IASI.

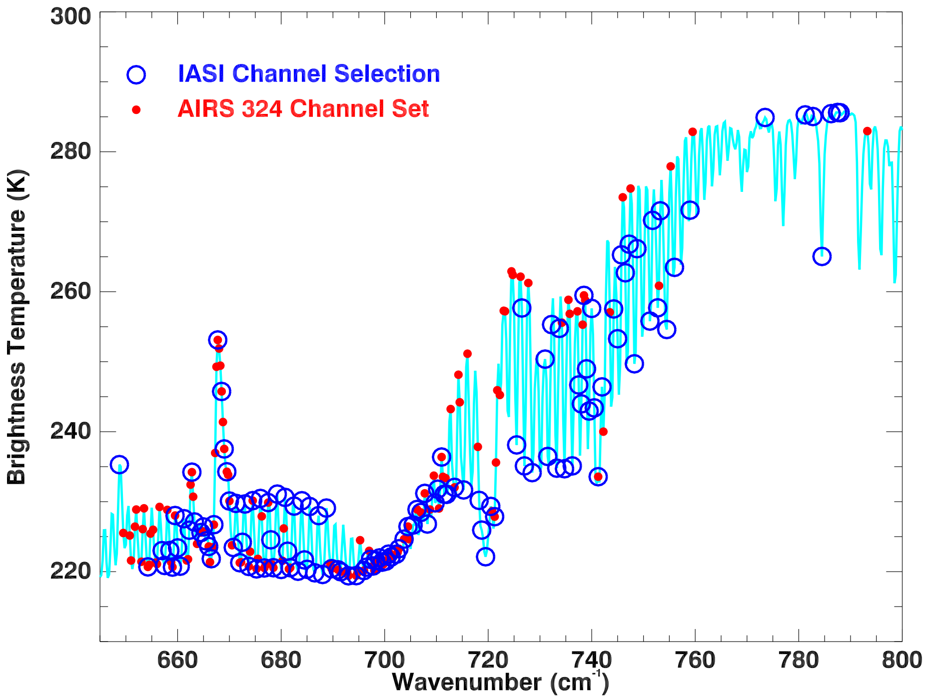

Fig. 8: As Figure 7, except focusing on the 15µm CO_2 *band.*

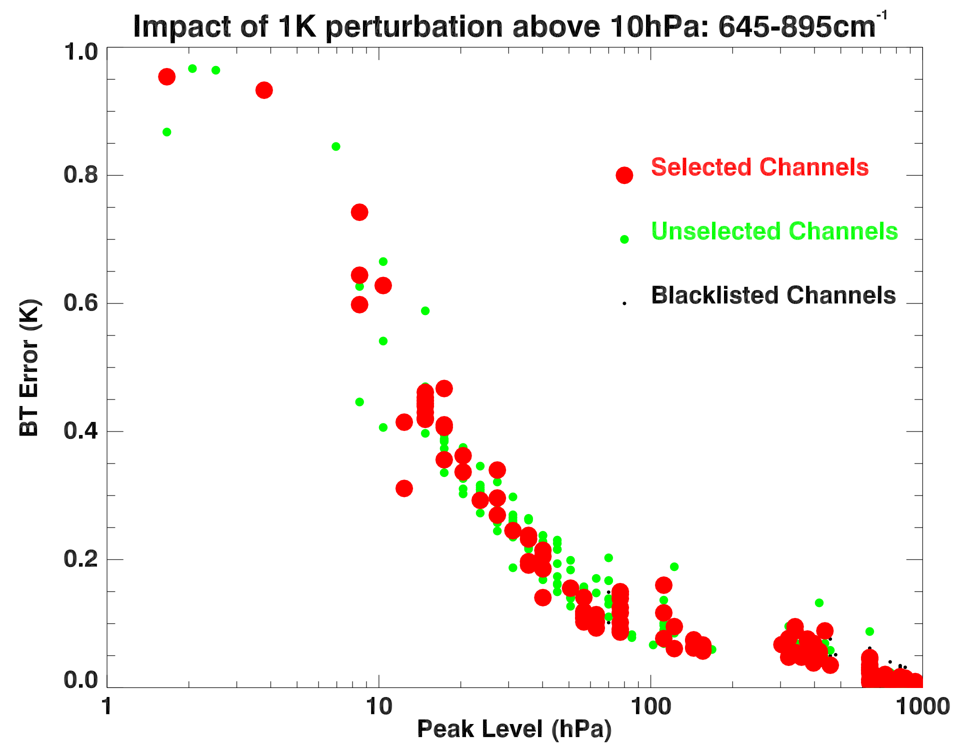

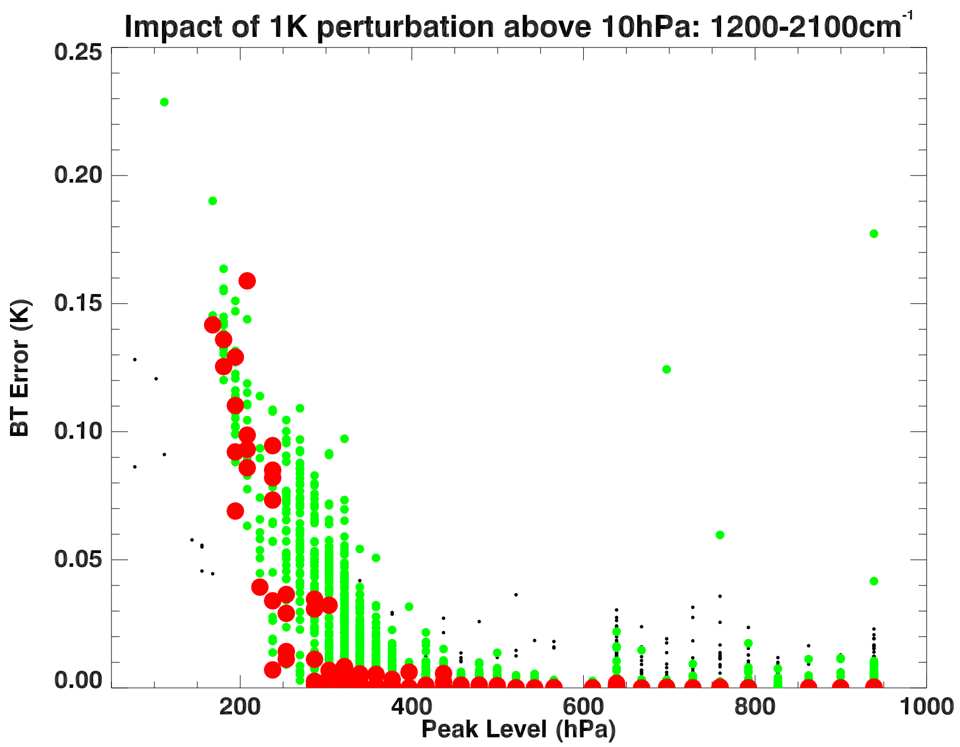

Fig. 9a (top) and 9b (bottom): The impact of a 1K temperature perturbation for all levels above 10hPa on the observed brightness temperature as a function of the level of the Jacobian peak for the main temperature and water vapour sounding regions of the spectrum. The large dots are the channels in this selection, the medium dots are those channels available for selection but not chosen; and the small dots are blacklisted channels.

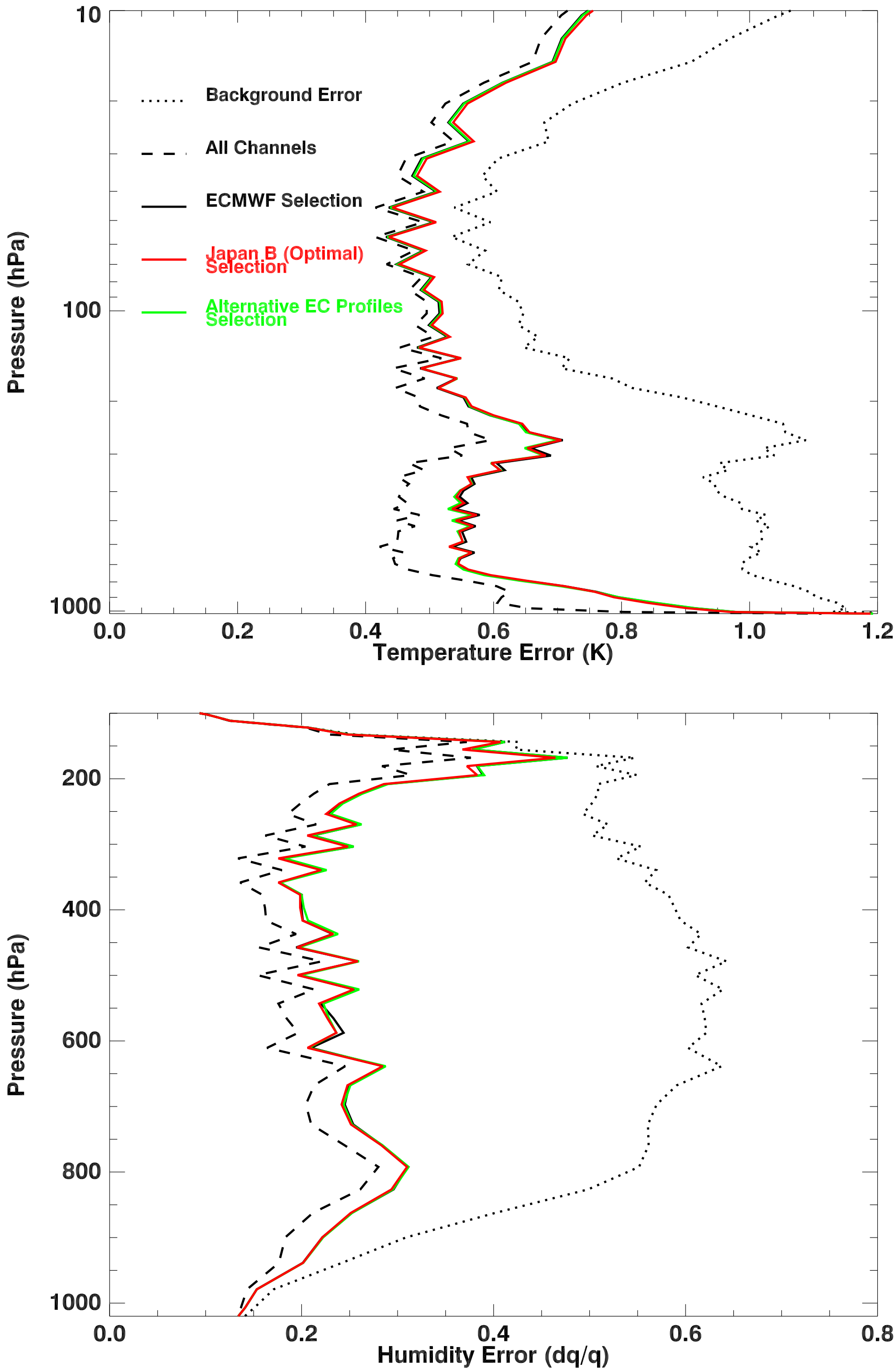

Fig. 10: Analysis errors for the U.S. Standard atmosphere and the JMA B-matrix on using all the channels; the optimal selection of 300 channels for the ECMWF B-matrix and the AFGL profile dataset; the optimal selection for the JMA ATOVS 1DVar B-matrix; and the optimal selection for the ECMWF B-matrix and an alternate set of atmospheric profiles.

4.2 Robustness of the channel selection.

The robustness of the algorithm is addressed with respect to its dependence on the assumed background error covariance matrix and also on its dependence of the atmospheric profiles being considered. It is tested by performing the channel selection for alternate scenarios (i.e., different B-matrix or different atmospheric profiles) and recomputing the DFS's that would result from the alternate channel sets but for the original scenario. That is, the detailed channel selection may well be different in the alternate scenarios but what is tested is whether the alternate channel selection contains similar information to the original when considered for the same profile and B-matrix.

The alternate B-matrix used was supplied by K. Okamoto (*priv. comm.*) and is based on the B-matrix used for ATOVS 1DVar pre-processing at JMA. On using this different B-matrix, the DFS after the temperature channels pre-selection was 73.6 (i.e., 6.1 per profile) rather than 75.5 for the optimal case. After the main run the respective values were 163.0 and 165.4 (i.e., a difference of 0.2 per profile). Out of the 252 channels chosen in each case 167 (66%) were common to both selections.

Seven alternate atmospheric profiles are taken from the Chevallier dataset and are chosen to cover a representative set of possible atmospheric states. In this case the DFS was 53.5 for the temperature channels pre-selection rather than the optimal 53.3. For the main run the values were 145.2 and 148.0 respectively. 180 channels were common to both selections.

The impact of these different selections on the expected analysis errors for the U.S. Standard atmosphere and the ECMWF B-matrix are shown in Figure 10.

While, as expected, there is some loss of information on changing the selection scenarios, these losses are relatively small and indicate that the channel selection is robust enough to serve as a global channel selection set.

The final set of 300 channels is given in Appendix A.

5 Summary of channel selection.

A selection of IASI channels has been determined based on the ECMWF background error covariance matrix. Channels have been chosen based on their information content (degrees of freedom for signal) derived from a linear analysis, but with the non-linear effects of the change in Jacobians for variable species being accounted for. The robustness of the selection has been explored with respect to the assumed atmospheric states and the background error covariance matrix.

It is necessary to combine the automatic channel selection algorithm of Rogers (1997, 2002) with manual intervention not only to mitigate the effects of non-linearity but also to ensure that the selection is as close to optimal as possible in various circumstances (e.g., daytime versus nighttime) and to allow for effects that are difficult to explicitly include in the algorithm (correlated error from surface emissivity).

Acknowledgements

This report is based on work carried out through EUMETSAT Contract No. EUM WP 989-2 (Collard and Matricardi, 2005). The following have provided input and feedback during this study: Tony McNally, Marco Matricardi, Fiona Hilton, John Eyre, Jean-Noël Thépaut, George Aumann, Chris Barnet, Alain Chédin, Louis

Garand, Reinhold Hess, Allen Huang, Bob Knuteson, Nadia Fourrié, Florence Rabier, Alan Lipton, Kozo Okamoto, Peter Rayer, Peter Schlüssel, Roger Saunders, Tim Schmidt, Bill Smith and Claudia Stubenrauch.

References

CHALON, G., F. CAYLA AND D. DIEBEL (2001). IASI: An Advanced Sounder for Operational Meteorology. *Proceedings of the 52nd Congress of IAF, Toulouse France, 1-5 Oct. 2001*

CHEVALLIER, F. (1999). TIGR-like sampled databases of atmospheric profiles from the ECMWF 50-level forecast model. *NWPSAF Research Report No. 1.*

CHEVALLIER, F., A. CHÉDIN, F. CHÉRUY AND J.J. MORCRETTE (2000). TIGR-like atmospheric profile databases for accurate radiative flux computation. *Q.J.R. Meteorol. Soc.*, **126**, 777–785.

COLLARD, A., AND M. MATRICARDI. Definition of an efficient interface to NWP for assimilating IASI radiances. *Report EUMETSAT Contract EUM/WP/989-2, ECMWF, Reading. 41pp.*

CREVOISIER, C, A. CHÉDIN AND N.A. SCOTT (2003). AIRS channel selection for CO_2 and other trace gas retrievals. *Q.J.R. Meteorol. Soc.*, **129**, 2719–2740.

ENGELEN, R.J., G.L. STEPHENS, AND A.S. DENNING. (2001). The effect of CO_2 variability on the retrieval of atmospheric temperatures. *Geophys. Res. Lett.*, **28**, 3259–3262.

FOURRIÉ, N. AND J.-N. THÉPAUT (2003). Evaluation of the AIRS near-real-time channel selection for application to numerical weather prediction. *Q.J.R. Meteorol. Soc.*, **129**, 2425–2439.

HUANG, H.-L., W.L. SMITH, J. LI, P. ANTONELLI, X. WU, R.O. KNUTESON, B. HUANG, AND B.J. OSBORNE (2004). Minimum local emissivity variance retrieval of cloud altitude and effective spectral emissivity — Simulation and initial verification. *J. Appl. Meteor.*, **43**, 795–809.

LIPTON, A.E. (2003). Satellite sounding channel optimization in the microwave spectrum. *IEEE T Geosci Remote*, **41**, 761–781.

MATRICARDI, M. (2003). RTIASI-4, a new version of the ECMWF fast radiative transfer model for the Infrared Atmospheric Sounding Interferometer. *ECMWF Technical Memorandum No. 425.*

MATRICARDI, M. (2004). The inclusion of aerosols and clouds in RTIASI. *Report EUMETSAT Contract EUM/CO/02/989/PS, ECMWF, Reading. 57pp.*

MATRICARDI, M. AND R. SAUNDERS (1999). Fast radiative transfer model for simulations of Infrared Atmospheric Sounding Interferometer radiances. *Appl. Optics*, **38**, 5679–5691.

RABIER, F., N. FOURRIÉ, D. CHAFAÏ AND P. PRUNET (2002). Channel selection methods for Infrared Atmospheric Sounding Interferometer radiances. *Q.J.R. Meteorol. Soc.*, **128**, 1011–1027.

RIZZI, R., M. MATRICARDI AND F. MISKOLCZI (2002). On the simulation of up-looking and down-looking high-resolution radiance spectra using two diverse line-by-line codes. *Appl. Optics*, **41**, 940–956.

RODGERS, C.D. (1996). Information content and optimisation of high spectral resolution measurements. *SPIE, 2380, Optical spectroscopic techniques and instrumentation for atmospheric and space research II, Paul B. Hays and Jinxue Wang eds.*, pp. 136–147.

RODGERS, C.D. (2000). Inverse methods for atmospheres: Theory and Practice. *World Scientific Publishers, Singapore.*

SUSSKIND, J., C.D. BARNET, AND J.M. BLAISDELL (2003). Retrieval of atmospheric and surface parameters from AIRS/AMSU/HSB data in the presence of clouds. *IEEE Trans. Geosci. Remote Sensing*, **41**, 390–409.

TJEMKES S.A., T. PATTERSON, R. RIZZI, M.W. SHEPHARD, S.A. CLOUGH, M. MATRICARDI, J.D. HAIGH, M. HOEPFNER, S. PAYAN, A. TROTSENKO, N. SCOTT, P. RAYER, J.P. TAYLOR, C. CLERBAUX, L.L. STROW, S. DESOUZA-MACHADO, D. TOBIN, R. KNUTESON (2003). The ISSWG line-by-line inter-comparison experiment. *J. Quant. Spectrosc. Radiat. Transfer*, **77**, 433–453.

Appendix: A 300 Channel Selection.

The 300 channels chosen by the example selection in this paper. Channels marked "Temp" were derived in the initial temperature pre-selection; Main refers to the main run and "Window" were the additional channels added to ensure cloud and emissivity effects are allowed for (Window/CO_2 and Window/H_2O are on weak absorption lines). The numbers indicate the order in which the channels were chosen within each run.

Chan	Waveno.	Notes
16	648.75	Main 63
38	654.25	Main 179
49	657.00	Main 153
51	657.50	Main 167
55	658.50	Main 165
57	659.00	Main 121
59	659.50	Main 180
61	660.00	Main 134
63	660.50	Main 130
66	661.25	Main 156
70	662.25	Main 160
72	662.75	Temp 15
74	663.25	Main 122
79	664.50	Main 149
81	665.00	Main 97
83	665.50	Main 144
85	666.00	Main 78
87	666.50	Temp 18
89	667.00	Temp 11
92	667.75	Temp 2
95	668.50	Temp 5
97	669.00	Temp 7
99	669.50	Temp 10
101	670.00	Main 73
104	670.75	Main 58
106	671.25	Main 100
109	672.00	Main 70
111	672.50	Main 90
113	673.00	Main 68

Chan	Waveno.	Notes
116	673.75	Main 50
119	674.50	Main 39
122	675.25	Main 29
125	676.00	Temp 24
128	676.75	Main 35
131	677.50	Main 45
133	678.00	Main 128
135	678.50	Temp 27
138	679.25	Temp 30
141	680.00	Temp 16
144	680.75	Main 31
146	681.25	Main 113
148	681.75	Temp 21
151	682.50	Main 55
154	683.25	Temp 13
157	684.00	Main 87
159	684.50	Main 103
161	685.00	Main 43
163	685.50	Main 105
167	686.50	Temp 23
170	687.25	Main 116
173	688.00	Main 32
176	688.75	Main 175
180	689.75	Main 56
185	691.00	Main 83
187	691.50	Main 65
193	693.00	Main 37
199	694.50	Temp 22
205	696.00	Temp 28

Chan	Wavenumber	Notes
207	696.50	Main 98
210	697.25	Main 177
212	697.75	Main 42
214	698.25	Main 161
217	699.00	Main 115
219	699.50	Main 49
222	700.25	Main 141
224	700.75	Main 95
226	701.25	Main 61
230	702.25	Main 76
232	702.75	Main 91
236	703.75	Main 106
239	704.50	Main 69
243	705.50	Temp 17
246	706.25	Main 84
249	707.00	Temp 25
252	707.75	Temp 29
254	708.25	Temp 43
260	709.75	Temp 45
262	710.25	Temp 35
265	711.00	Temp 32
267	711.50	Temp 40
269	712.00	Temp 47
275	713.50	Temp 14
282	715.25	Temp 49
294	718.25	Temp 42
296	718.75	Temp 36
299	719.50	Main 152
303	720.50	Temp 20
306	721.25	Temp 39
323	725.50	Temp 64
327	726.50	Temp 53
329	727.00	Temp 61
335	728.50	Temp 57
345	731.00	Temp 3
347	731.50	Temp 50
350	732.25	Temp 38
354	733.25	Temp 55
356	733.75	Temp 44
360	734.75	Temp 58
366	736.25	Temp 59
371	737.50	Temp 63
373	738.00	Temp 54
375	738.50	Temp 41
377	739.00	Temp 60
379	739.50	Temp 52
381	740.00	Temp 26

Chan	Wavenumber	Notes
383	740.50	Temp 34
386	741.25	Temp 33
389	742.00	Temp 37
398	744.25	Temp 8
401	745.00	Temp 12
404	745.75	Temp 62
407	746.50	Temp 65
410	747.25	Temp 48
414	748.25	Temp 46
416	748.75	Temp 19
426	751.25	Temp 66
428	751.75	Temp 9
432	752.75	Temp 51
434	753.25	Temp 4
439	754.50	Temp 6
445	756.00	Temp 56
457	759.00	Temp 31
515	773.50	Main 109
546	781.25	Main 12
552	782.75	Main 26
559	784.50	Main 119
566	786.25	Main 86
571	787.50	Main 54
573	788.00	Main 137
646	806.25	Window/CO_2
662	810.25	Main 183
668	811.75	Main 159
756	833.75	Window
867	861.50	Window
906	871.25	Window/H_2O
921	875.00	Window
1027	901.50	Window
1046	906.25	Window/H_2O
1121	925.00	Window/H_2O
1133	928.00	Window
1191	942.50	Window/CO_2
1194	943.25	Window
1271	962.50	Window
1479	1014.50	Ozone 5
1509	1022.00	Ozone 4
1513	1023.00	Ozone 2
1521	1025.00	Ozone 1
1536	1028.75	Ozone 11
1574	1038.25	Ozone 15
1579	1039.50	Ozone 10
1585	1041.00	Ozone 13
1587	1041.50	Ozone 6

Chan	Waveno.	Notes
1626	1051.25	Ozone 3
1639	1054.50	Ozone 7
1643	1055.50	Ozone 8
1652	1057.75	Ozone 12
1658	1059.25	Ozone 14
1671	1062.50	Ozone 9
1786	1091.25	Window/H_2O
1805	1096.00	Window
1884	1115.75	Window
1991	1142.50	Window
2019	1149.50	Window/H_2O
2094	1168.25	Window
2119	1174.50	Main 154
2213	1198.00	Main 88
2239	1204.50	Temp 1
2271	1212.50	Main 129
2321	1225.00	Main 57
2398	1244.25	Main 72
2701	1320.00	Main 126
2741	1330.00	Main 145
2819	1349.50	Main 140
2889	1367.00	Main 8
2907	1371.50	Main 33
2910	1372.25	Main 114
2919	1374.50	Main 157
2939	1379.50	Main 47
2944	1380.75	Main 53
2948	1381.75	Main 176
2951	1382.50	Main 108
2958	1384.25	Main 17
2977	1389.00	Main 107
2985	1391.00	Main 136
2988	1391.75	Main 150
2991	1392.50	Main 23
2993	1393.00	Main 11
3002	1395.25	Main 6
3008	1396.75	Main 123
3014	1398.25	Main 60
3027	1401.50	Main 77
3029	1402.00	Main 52
3036	1403.75	Main 59
3047	1406.50	Main 184
3049	1407.00	Main 3
3053	1408.00	Main 135
3058	1409.25	Main 93
3064	1410.75	Main 117
3069	1412.00	Main 71

Chan	Wavenumber	Notes
3087	1416.50	Main 185
3093	1418.00	Main 14
3098	1419.25	Main 13
3105	1421.00	Main 2
3107	1421.50	Main 46
3110	1422.25	Main 18
3127	1426.50	Main 170
3136	1428.75	Main 169
3151	1432.50	Main 94
3160	1434.75	Main 27
3165	1436.00	Main 38
3168	1436.75	Main 44
3175	1438.50	Main 81
3178	1439.25	Main 146
3207	1446.50	Main 111
3228	1451.75	Main 162
3244	1455.75	Main 1
3248	1456.75	Main 22
3252	1457.75	Main 7
3256	1458.75	Main 85
3263	1460.50	Main 104
3281	1465.00	Main 110
3303	1470.50	Main 125
3309	1472.00	Main 143
3312	1472.75	Main 15
3322	1475.25	Main 41
3375	1488.50	Main 92
3378	1489.25	Main 181
3411	1497.50	Main 21
3438	1504.25	Main 132
3440	1504.75	Main 147
3442	1505.25	Main 151
3444	1505.75	Main 89
3446	1506.25	Main 4
3448	1506.75	Main 19
3450	1507.25	Main 82
3452	1507.75	Main 20
3454	1508.25	Main 164
3458	1509.25	Main 102
3467	1511.50	Main 178
3476	1513.75	Main 139
3484	1515.75	Main 62
3491	1517.50	Main 168
3497	1519.00	Main 79
3499	1519.50	Main 173
3504	1520.75	Main 101
3506	1521.25	Main 186

Chan	Waveno.	Notes
3509	1522.00	Main 34
3518	1524.25	Main 155
3527	1526.50	Main 112
3555	1533.50	Main 127
3575	1538.50	Main 30
3577	1539.00	Main 131
3580	1539.75	Main 9
3582	1540.25	Main 120
3586	1541.25	Main 66
3589	1542.00	Main 163
3599	1544.50	Main 124
3653	1558.00	Main 36
3658	1559.25	Main 51
3661	1560.00	Main 64
4032	1652.75	Main 174
5368	1986.75	Main 138
5371	1987.50	Main 148
5379	1989.50	Main 24
5381	1990.00	Main 5
5383	1990.50	Main 40
5397	1994.00	Main 96
5399	1994.50	Main 16
5401	1995.00	Main 28
5403	1995.50	Main 48
5405	1996.00	Main 118
5455	2008.50	Main 171
5480	2014.75	Main 10

Chan	Wavenumber	Notes
5483	2015.50	Main 67
5485	2016.00	Main 172
5492	2017.75	Main 80
5502	2020.25	Main 99
5507	2021.50	Main 158
5509	2022.00	Main 75
5517	2024.00	Main 133
5558	2034.25	Main 182
5988	2141.75	Main 142
5992	2142.75	Main 74
5994	2143.25	Main 25
6003	2145.50	Main 166
6982	2390.25	Solar 13
6985	2391.00	Solar 11
6987	2391.50	Solar 9
6989	2392.00	Solar 7
6991	2392.50	Solar 5
6993	2393.00	Solar 8
6995	2393.50	Solar 4
6997	2394.00	Solar 12
7267	2461.50	Solar 3
7269	2462.00	Solar 1
7424	2500.75	Solar 2
7426	2501.25	Solar 6
7428	2501.75	Solar 10
7885	2616.00	Window
8007	2646.50	Window